

# Myenteric neurons of the mouse small intestine undergo significant electrophysiological and morphological changes during postnatal development

Jaime Pei Pei Foong<sup>1,2</sup>, Trung V. Nguyen<sup>2</sup>, John B. Furness<sup>2</sup>, Joel C. Bornstein<sup>1</sup> and Heather M. Young<sup>2</sup>

Departments of <sup>1</sup>Physiology and <sup>2</sup>Anatomy & Cell Biology, University of Melbourne, Parkville, Victoria 3010, Australia

## Key points

- Different functional types of neurons within the gut wall form circuits that regulate intestinal motility.
- To examine the postnatal development of electrical properties of different classes of enteric neurons, we performed intracellular recordings from neurons in the mouse duodenum at three ages: postnatal day (P)0, P10–11 and adult.
- Like adults, two main morphological classes of neurons are present at P0 and P10–11. P0 and P10–11 neurons with Dogiel type II (DII) morphology had multiple long processes that achieved their adult projection length by P10–11. However, they differed electrophysiologically from adult DII neurons in that they displayed prominent afterdepolarizing potentials.
- Most electrical properties of neurons with a single long process were mature by P10–11. However, these neurons showed significant postnatal changes in morphology and projection length.
- Major morphological and electrophysiological changes in enteric neurons occur postnatally, which could underlie changes in gut motility during development.

**Abstract** Organized motility patterns in the gut depend on circuitry within the enteric nervous system (ENS), but little is known about the development of electrophysiological properties and synapses within the ENS. We examined the electrophysiology and morphology of myenteric neurons in the mouse duodenum at three developmental stages: postnatal day (P)0, P10–11, and adult. Like adults, two main classes of neurons could be identified at P0 and P10–11 based on morphology: neurons with multiple long processes that projected circumferentially (Dogiel type II morphology) and neurons with a single long process. However, postnatal Dogiel type II neurons differed in several electrophysiological properties from adult Dogiel type II neurons. P0 and P10–11 Dogiel type II neurons exhibited very prominent  $\text{Ca}^{2+}$ -mediated afterdepolarizing potentials (ADPs) following action potentials compared to adult neurons. Adult Dogiel type II neurons are characterized by the presence of a prolonged afterhyperpolarizing potential (AHP), but AHPs were very rarely observed at P0. The projection lengths of the long processes of Dogiel type II neurons were mature by P10–11. Uniaxonal neurons in adults typically have fast excitatory postsynaptic potentials (fEPSPs, ‘S-type’ electrophysiology) mainly mediated by nicotinic receptors. Nicotinic-fEPSPs were also recorded from neurons with a single long process at P0 and P10–11. However, these neurons underwent major developmental changes in morphology, from predominantly filamentous neurites at birth to lamellar dendrites in mature mice. Unlike Dogiel type II neurons, the projection lengths of neurons with a single long process matured

after P10–11. Slow EPSPs were rarely observed in P0/P10–11 neurons. This work shows that, although functional synapses are present and two classes of neurons can be distinguished electrophysiologically and morphologically at P0, major changes in electrophysiological properties and morphology occur during the postnatal development of the ENS.

(Received 8 December 2011; accepted after revision 21 February 2012; first published online 27 February 2012)

**Corresponding author** J. P. P. Foong: Department of Physiology, University of Melbourne, Parkville, Victoria 3010, Australia. Email: j.foong@unimelb.edu.au

**Abbreviations** ADP, afterdepolarizing potential; AHP, afterhyperpolarizing potential; DII, Dogiel type II; ENS, enteric nervous system; fEPSP, fast EPSP.

## Introduction

The enteric nervous system (ENS) is the complex network of neurons and glia within the wall of the gastrointestinal tract that regulates motility, water and electrolyte secretion, and local blood flow (Langley, 1921; Gershon, 1998; Furness, 2006). Multiple functional subtypes of myenteric neuron (motor neurons, interneurons and sensory neurons) have been identified, but they can be broadly separated into two classes based on their electrophysiological properties and morphologies (Bornstein *et al.* 1994). AH neurons display long after-hyperpolarizing potentials (AHPs) following action potentials, and have a smooth cell body and multiple axons, referred to as Dogiel type II (DII) morphology (Furness *et al.* 1998). S-type neurons exhibit fast EPSPs (fEPSPs) in response to stimulation of fibre tracts and do not exhibit AHPs (Hirst *et al.* 1974; Gwynne & Bornstein, 2007). S-neurons are uniaxonal, and most have lamellar dendrites in the mouse (Nurgali *et al.* 2004), as in other species.

The ENS arises predominantly from the vagal neural crest. In the mouse, vagal neural crest-derived cells enter the foregut at embryonic day (E)9.5 and then migrate along the wall of the gastrointestinal tract in a rostral-to-caudal wave. The full length of the gut is colonized by neural crest-derived cells by E14.5 (Kapur *et al.* 1992). The processes of migration, proliferation and differentiation of enteric neuron precursors have been studied extensively (Hao & Young, 2009; Gershon, 2010), but there are few data on the maturation of electrophysiological properties of enteric neurons. While neural crest-derived cells are colonizing the gut, a subpopulation starts to differentiate into neurons as shown by the expression of pan-neuronal markers (Baetge & Gershon, 1989; Young *et al.* 1999). A recent study showed that, following dissociation and short-term culture, enteric neurons from the gut of E11.5–E12.5 mice show spontaneous and electrically stimulated  $\text{Ca}^{2+}$  transients, respond to ATP and nicotinic agonists, and can fire action potentials (Hao *et al.* 2011). However, neurally mediated spontaneous propagating motility patterns are not present until just prior to birth (E18.5) in the mouse duodenum, and after birth in the colon (Roberts *et al.* 2007, 2010). As the circuitry mediating neurally mediated motility

patterns involves synapses between different types of neurons, it might be assumed that the electrophysiological properties of neurons and functional synapses present at birth in mouse duodenum are similar to those in the adult. However, it is not currently known what electrophysiological types of enteric neurons are present at birth, whether there are functional synapses between enteric neurons, and whether there are any changes in the electrophysiological and morphological properties of neurons during postnatal development.

In this study, we used conventional intracellular recording methods to record from myenteric neurons from the small intestine of early postnatal (postnatal day (P)0, P10–11) and adult mice to examine electrophysiological properties, synaptic transmission and morphology. We found that both DII and neurons with a single long process were present by P0. However, both types of neuron underwent significant changes in electrophysiological properties and synaptic inputs during postnatal development. S-type neurons also underwent major morphological alterations.

## Methods

### Experimental animals

Experiments were performed on the duodenum of P0, P10 and P11 or adult C57BL/6 mice. Mice were killed by cervical dislocation (P10–11, adults), or decapitation (P0) in accordance with the approval of the Anatomy & Cell Biology, Neuroscience, Pathology, Pharmacology, and Physiology Animal Experimentation Ethics Committee of the University of Melbourne. All experiments conform with *The Journal of Physiology* policy on animal experimentation (Drummond, 2009). The proximal duodenum (1.0–2.5 cm segment of duodenum distal to the pylorus) was removed and immediately placed in physiological saline (composition in mM: NaCl 118,  $\text{NaHCO}_3$  25, D-glucose 11, KCl 4.8,  $\text{CaCl}_2$  2.5,  $\text{MgSO}_4$  1.2,  $\text{NaH}_2\text{PO}_4$  1.0; containing 2.5  $\mu\text{M}$  nicardipine and 1  $\mu\text{M}$  hyoscine), bubbled with 95%  $\text{O}_2$ –5%  $\text{CO}_2$ . For P0 and P10–P11 tissues, the duodenal segments were cut along the mesenteric border, and the mucosa and submucosa

were removed from the underlying smooth muscle and myenteric plexus layers. The smooth muscle and myenteric plexus preparation was then pinned flat, serosa side up, in an organ bath lined with a silicone elastomer (Sylgard 184, Dow Corning, North Ryde, NSW, Australia). Adult preparations of duodenum and ileum were dissected from segments that were opened along the mesenteric border and pinned flat, mucosa up, in a Sylgard dissecting dish. The mucosa and submucosa were removed, and some circular muscle was dissected away from the myenteric plexus leaving the longitudinal muscle intact. Preparations were then transferred to a recording chamber and pinned serosa down to allow impalements from the circular muscle side. All preparations were continually superfused with physiological saline (33–34°C) bubbled with 95% O<sub>2</sub>–5% CO<sub>2</sub>, and left to equilibrate for 1 h before beginning the electrophysiological experiments.

### Electrophysiology

Conventional intracellular recording techniques were used to impale and record from myenteric neurons. Myenteric ganglia were viewed at  $\times 200$  magnification using an Olympus inverted microscope (Olympus IX70). Intracellular microelectrodes (100–200 M $\Omega$ ) containing 1 M KCl and 2% biocytin (Sigma Aldrich, Castle Hill, NSW, Australia) were used. The excitability of impaled neurons was examined by applying depolarizing current pulses (500 ms duration, 50–300 pA amplitude) in 10 pA increments, at resting membrane potential (RMP) or by holding the membrane potential at  $-60$  mV. Hyperpolarizing current pulses (500 ms, 50–300 pA,  $-10$  pA increments) were applied to examine for the presence of  $I_h$  currents and anode break action potentials and to obtain data for input resistance measurements.  $I_h$  currents were identified as a time-dependent reduction in the membrane potential change in response to a hyperpolarizing current pulse.

Synaptic potentials displayed by myenteric neurons were examined by applying either a single focal electrical stimulus (typically 0.4–1.8 mA, 1 ms) or trains of stimuli (3 or 10 pulses, 20 Hz) via a monopolar stimulating electrode (50  $\mu$ m, non-insulated tungsten wire) placed on an interganglionic fibre tract leading into the ganglion containing the impaled cell, oral or circumferential to the impaled cell region.

### Drugs used

Hyoscine hydrobromide, hexamethonium bromide and nicardipine (all Sigma-Aldrich) were prepared as 1000-fold stock solutions dissolved in distilled water, and diluted to their final concentrations in physiological saline before addition to the organ bath.

### Data measurements and statistics

Electrophysiological data were recorded and analysed with Axoscope 10.2.0.14 software (Axon Instruments, Union City, CA, USA). The excitability of cells was analysed by measuring the action potential threshold, and counting the maximum number of action potentials triggered by depolarizing current pulses. The instantaneous frequency of firing was measured as the inverse of the duration between the first two action potentials fired at the beginning of the depolarizing current pulse. The total action potential burst frequency was measured as the maximum number of action potentials divided by the duration between the first and last action potential peaks in that burst. The input resistance of neurons was obtained from line of best fit (linear regression) to an  $I$ – $V$  plot. The membrane potential (resting membrane potential or membrane potential held at  $-60$  mV) of an impaled neuron immediately before a stimulus was used as the baseline. The amplitude of action potentials (from the baseline to the peak) and half-duration of an action potential (width at half maximum peak amplitude) were measured. Due to technical difficulty, some of these parameters were not analysed in P0 neurons.

The maximum change in amplitude and the total duration of responses or synaptic potentials evoked by stimulation of interganglionic fibre tracts were analysed. Fast excitatory postsynaptic potentials (fEPSPs) and other responses (where noted) were recorded at a holding potential of  $-100$  mV. The maximum peak amplitude, number of peaks and duration of stimulated fEPSP complexes were measured. The maximum peak amplitude and number of peaks were measured for non-stimulus-locked fEPSPs. Each stimulus regime was repeated at least three times to obtain an average value for each parameter of each cell. For pharmacological experiments, the mean values of relevant parameters were obtained in control, drug (following a wash-in period of 6–10 min) and, where possible, wash-out conditions for statistical comparison.

All results are presented as means  $\pm$  SEM. Statistical comparisons were performed using Student's unpaired  $t$  test (2-tailed), one-way ANOVA with the Tukey–Kramer test for multiple group comparisons or a  $\chi^2$  test with 1 or 2 degrees of freedom (df);  $P$  values less than 0.05 were considered to be significant.

### Localization of biocytin

Impaled neurons were filled with biocytin during intracellular recordings. After electrophysiological experiments, the preparation was fixed overnight in 4% formaldehyde in 0.1 M phosphate buffer, pH 7.2 at 4°C. The tissue was then given three washes with phosphate buffered saline (PBS), followed by a 30 min incubation

with 1% Triton X-100 (ProSciTech, Thuringowa, QLD, Australia). After three washes with PBS, the preparation was incubated for  $\sim 2.5$  h with Steptavidin Alexa Fluor 594 (1:200; Molecular Probes, Mulgrave, Vic, Australia). The tissue was given another three washes with PBS, and then mounted on a slide. Images of the filled neurons were taken using a Zeiss Pascal confocal laser scanning microscope. Images of the cell bodies were surfaced rendered using Imaris software (Bitplane AG, Switzerland).

To aid in the analysis of the morphologies and projections of filled neurons, a permanent diaminobenzidine stain of some myenteric plexus preparations was obtained following confocal imaging as described previously (Clerc *et al.* 1998). Maintaining the impalement of a neuron for a long time (at least 20 min) provided good biocytin fills of their processes, indicated by expansion blubs formed at the tips of the processes where they were severed by dissection. To compare projection lengths of the neurons in relation to the growth of the duodenum at P0, P10–11 and adult, two parameters were measured: (1) the length of the small intestine from the pylorus to the ileo-caecal junction; (2) the circumference of stretched, pinned out preparations of duodenum.

## Results

Electrophysiological experiments were conducted on myenteric plexus preparations of P0 ( $n = 29$ ), P10–11 ( $n = 65$ ) and adult ( $n = 26$ ) duodenum. Experiments were also conducted on 18 myenteric plexus preparations of adult ileum to provide a comparison between gut regions. A total of 105 myenteric neurons were impaled from P10–11 mice, from which successful recordings were obtained from 92 neurons, and 65/92 neurons were identified with *post hoc* localization of biocytin. Thirteen P10–11 neurons were classified only by their morphology. A total of 40 neurons were impaled from P0 mice. Of these, electrophysiological recordings were obtained from 25 neurons, and 21/25 neurons were localized with biocytin and analysed morphologically. Fifteen neurons supplied morphological data only.

### Neuron morphology: Dogiel type II (DII) neurons and neurons with a single long process are present in the duodenum of newborn mice

Neurons could be classified by their morphologies at P0. Of 36 P0 neurons studied morphologically, 14 had smooth cell bodies with multiple long processes (DII morphology, Fig. 1A), and 22 had a single long (axon-like) process (Fig. 1D). At P10–11, 46/78 neurons displayed DII morphology (Fig. 1A), while 32/78 neurons had a single long process. In the adult, 18/38 myenteric neurons

in the duodenum, and 9/21 myenteric neurons in the ileum were DII; while 20/38 neurons in the duodenum and 12/21 neurons in the ileum were uniaxonal. There was no significant difference in the proportion of the two morphological classes of neurons at P0, P10–11 and adult duodenum ( $\chi^2$  test, 2 df,  $P = 0.1$ ). There was also no significant difference in the proportion between the duodenum and ileum of adult mice ( $\chi^2$  test, 1 df,  $P = 0.7$ ).

### DII neurons achieve mature projection lengths by P10–11

DII neurons possessed long processes that projected circumferentially around the gut (Fig. 1A). The circumferential projection lengths of DII neurons from the duodenum of P0 mice ( $590 \pm 80 \mu\text{m}$ ,  $n = 14$ ) were significantly smaller than those from P10–11 and adult mice ( $P = 0.0002$ ). At P10, the processes of some DII neurons projected around almost the entire circumference of the duodenum, and provided branches to many ganglia. Surprisingly, the circumferential projection lengths of DII neurons in the P10–11 duodenum were those of adult DII neurons (P10:  $1450 \pm 100 \mu\text{m}$ ,  $n = 37$ ; adult:  $1360 \pm 220 \mu\text{m}$ ,  $n = 16$ ,  $P > 0.05$ ; Fig. 1B). As the circumference of the duodenum increases by  $\sim 83\%$  between P10–11 and adult (P0: 0.4 cm, P10: 0.6 cm, adult: 1.1 cm,  $n = 4$  each,  $P < 0.0001$ ; Fig. 1B), these data show that the circumferential projection lengths of DII neurons during development did not increase in proportion to the circumference of the duodenum (Fig. 1B).

### Neurons with a single long process undergo significant increases in projection length after P10–11

Orally and anally projecting neurons with a single long process were present in the duodenum of P0 mice (Fig. 1D). Some circumferentially projecting neurons with a single long process were also observed at P10–11 (4/32 neurons). The mean lengths of projections of anally projecting neurons were not significantly different between P0 and P10–11, but significantly increased between P10–11 and adult ( $P = 0.0005$ , Fig. 1C). While a similar trend was observed for orally projecting neurons, the mean length of projections for these neurons was not significantly different between P0 and P10–11, between P10–11 and adult, or between P0 and adult (Fig. 1C). To compare the increase in projection length to the increase in length of the intestine, the length of the small intestine was measured at P0, P10–11 and adults (the length of the entire small intestine was measured because there is no distinct anatomical landmark marking the duodeno-jejunal junction in mice). The small intestine undergoes a significant increase in length during development (P0:  $6.8 \pm 0.1$  cm, P10  $14.9 \pm 0.9$  cm, adult

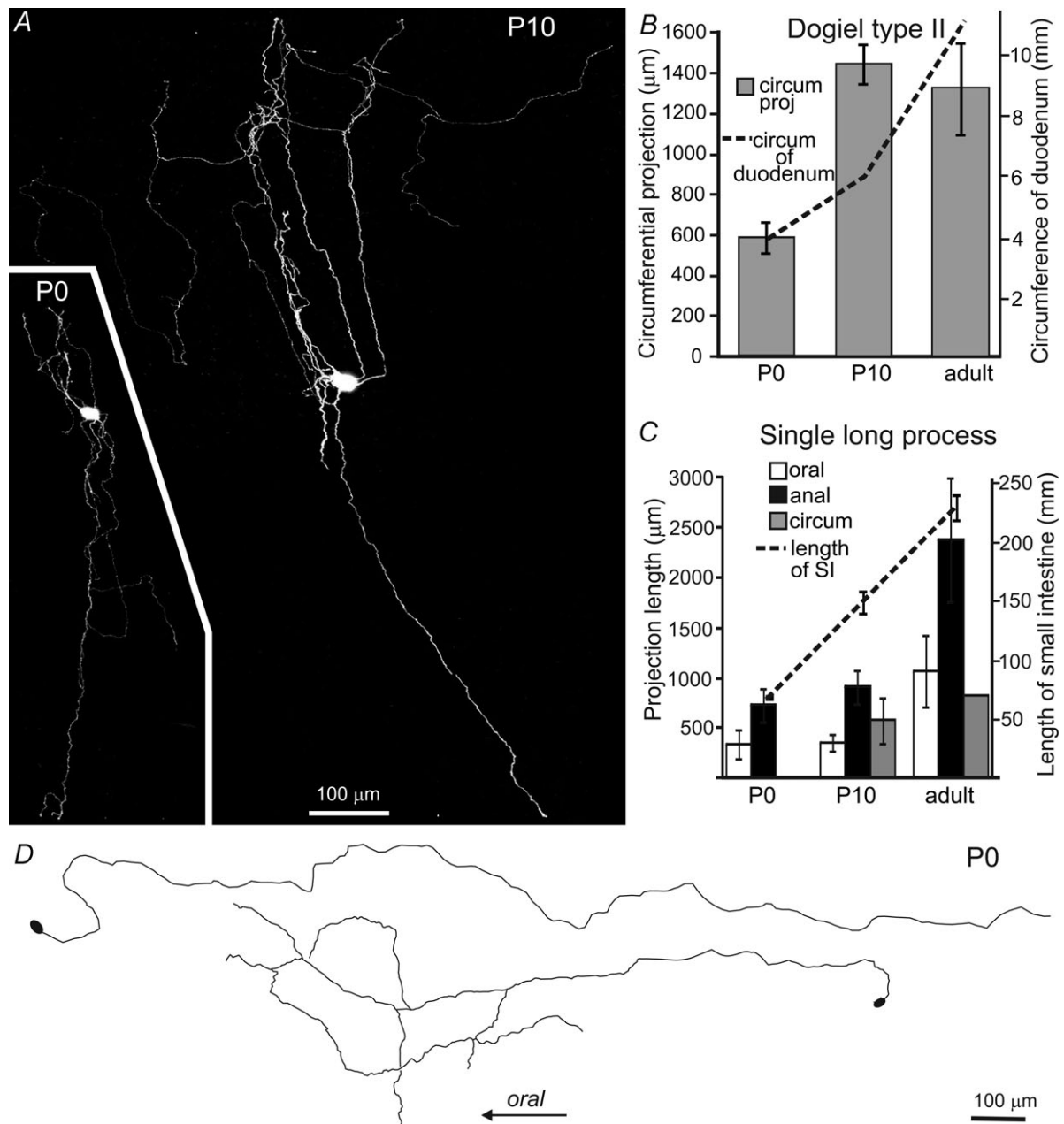


**Figure 1. Morphology of P0 and P10–11 myenteric neurons revealed by the injection of biocytin through the recording electrode**

A, neurons with smooth cell bodies and multiple processes (DII morphology) from the duodenum of P0 (inset) and P10–11 mice. The processes of some P10–11 DII neurons projected around almost the entire circumference of the gut. Neurons with DII morphology had prolonged AHPs (see also Fig. 3A and B). B, the circumferential projection lengths of DII neurons (grey bars, LHS y-axis). DIIs had reached their mature projection lengths by P10. The circumference of the duodenum (dotted line and RHS y-axis) also increased during development, but between P0 and P10–11, the projections of DII neurons grew faster than the increase in gut circumference. C, the longitudinal projection lengths of neurons with a single long process (bars, LHS y-axis). The projection lengths increased during development. The small intestine also grew significantly in length (dashed line, RHS y-axis). However, the increases in projection lengths of these neurons did not closely parallel the increase in length of the small intestine. D, traces of long orally and anally projecting neurons at P0. The orally projecting neuron shown was the longest orally projecting neuron we encountered at P0. P0 and P10–11 neurons with a single long process were found to display S-type electrophysiology.

$22.9 \pm 1.1$  cm,  $n = 4$  each,  $P < 0.0001$ ; Fig. 1C). However, the increase in mean projection length of neurons with a single long process did not parallel closely the increase in length of the small intestine, and between P0 and P10–11, the mean increase in projection length was less than the increase in the relative length of the small intestine (Fig. 1C).

### Early postnatal neurons with a single long process undergo significant changes in morphology

Most (13/18) adult uniaxonal duodenal neurons possessed only lamellar dendrites (Dogiel Type I morphology, Fig. 2H–L), while the remaining five neurons possessed both lamellar and filamentous dendrites (Fig. 2L). In contrast, in P0 mice, just 1 (of 18) neurons with a single long process examined had only lamellar neurites (Fig. 2C and L). These were very small and stumpy compared to the lamellar dendrites displayed by adult uniaxonal neurons

(Fig. 2H–K). Half (9/18) of the P0 neurons possessed only filamentous neurites (Fig. 2A), and eight neurons had both lamellar and filamentous neurites (Fig. 2L). By P10–11, the proportion of neurons possessing only filamentous neurites (Fig. 2E) had reduced to only 14% (3/21), while the proportion of neurons possessing only lamellar neurites (24%, 5/21, Fig. 2F–G) and both lamellar and filamentous neurites (62%, 13/21, Fig. 2D) had increased (Fig. 2L). The proportion of neurons expressing only lamellar dendrites increased significantly as the gut matures ( $P < 0.0001$ ,  $\chi^2$  test, 2 df).

In summary, these data show that during postnatal development: (1) neurons with a single long process undergo dramatic changes in morphology; (2) the mean increase in the circumferential projections of DII neurons and of orally and anally projecting neurons with a single long process do not parallel closely the increase in the circumference and length of the small intestine, respectively.

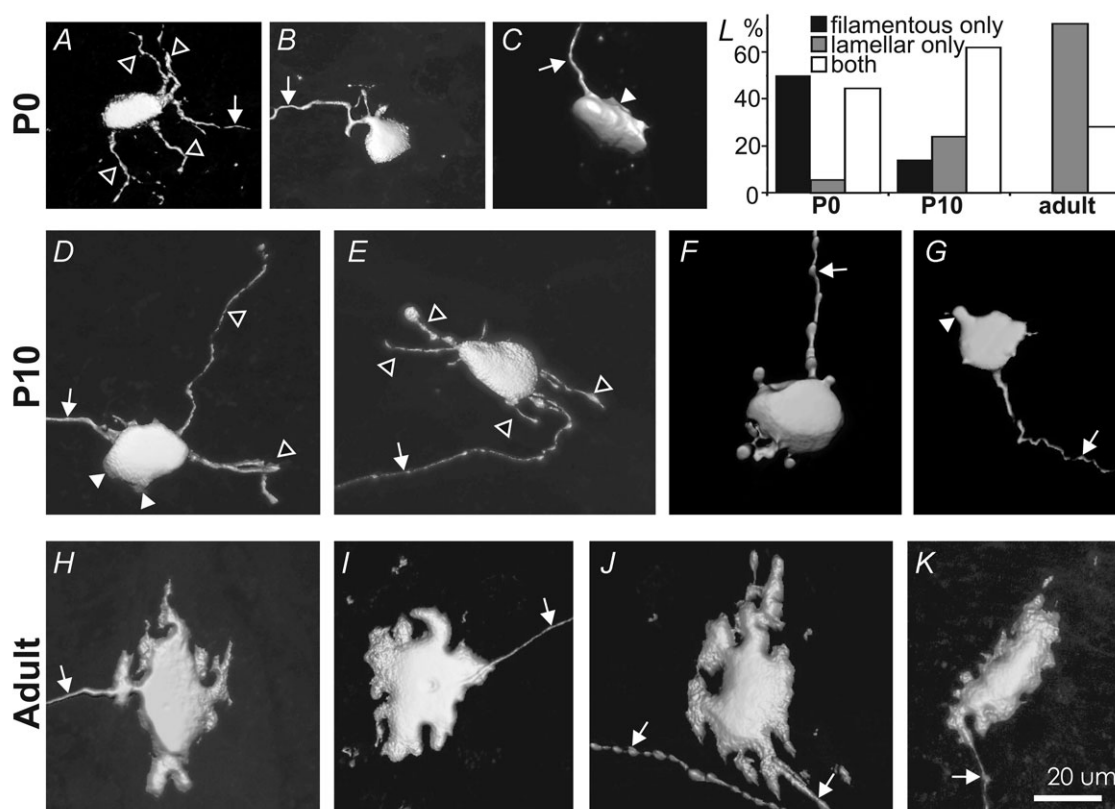


**Figure 2. Developmental changes in the morphology of biocytin-filled neurons with a single long process**

Surface rendering of projected confocal micrographs of neurons with a single long process (indicated by arrow) from the duodenum of P0, P10–11 and adult mice. At P0 and P10–11, neurons possessed only filamentous neurites (open arrow heads) (A and E), both filamentous (open arrow heads) and lamellar neurites (arrow heads) (B, D and F), or rarely, only lamellar neurites (arrow heads) (C and G). Compared to the prominent lamellar dendrites seen on adult neurons (H–K), the lamellar neurites of P0 neurons (arrow heads) were only small bumps on the soma. L, quantification of the proportions of neurons with a single long process with different morphologies. The proportion of neurons possessing only lamellar neurites increased from P0 to adult.

### Early postnatal neurons with prolonged AHPs display DII morphology

At P10–11, 35/92 neurons displayed a long AHP following action potentials, characteristic of AH-type electrophysiology (Fig. 3B). *Post hoc* localization of biocytin identified 32 out of the 35 neurons, and revealed that all 32 displayed DII morphology (Fig. 3B). Three other neurons recorded exhibited proximal process potentials, and they were also revealed to have DII morphology. At P0, only 1/25 neurons examined electrophysiologically displayed a long AHP and it was found to exhibit DII morphology (Fig. 3A). AHPs from P0 and P10–11 animals were only revealed following a train of action potentials evoked by a long depolarizing step current. In contrast, in adult neurons, a single action potential was often accompanied by a noticeable AHP (duodenum: 12/17 DII neurons, ileum: 9/9 DII neurons). The mean amplitude of AHPs recorded from adult duodenal DII neurons ( $2.8 \pm 0.5$  mV,  $n = 17$ ) were smaller than the amplitudes of AHPs recorded from the ileal neurons ( $5.2 \pm 0.7$  mV,  $n = 9$ ;  $P = 0.01$ ).

Although only 1/25 P0 neurons displayed a long AHP, 7/25 P0 neurons analysed electrophysiologically displayed DII morphology. Six of these P0 DII neurons displayed a depolarization following the action potential (after-depolarizing potential; ADP), which was also displayed by many P10–11 AH/DII neurons (see below), but not by any other neurons.

### Early postnatal DII neurons display more a prominent ADP compared to adult

Prominent ADPs were observed in P0 and P10–11 neurons following action potentials that were evoked via stimulation of internodal strands (Fig. 4B–C), injecting depolarizing step current (Fig. 4A), and/or anode break action potentials (Fig. 4D). Although spontaneous action potentials seldom occurred, ADPs were also observed after some spontaneous action potentials. ADPs were enhanced by hyperpolarization of membrane potential (reversal potential of  $-41$  mV; Fig. 4E), and were associated with an increase in membrane conductance (Fig. 1C). The rising phase of an ADP sometimes evoked several small action potentials (Fig. 4B).

At P10–11, ADPs were exclusively displayed by neurons that exhibited DII morphology, and/or long AHPs; the majority of these neurons (38/43) displayed ADPs. A further eight P10–11 neurons had ADPs, but their morphology is unknown. At P0, ADPs were also only recorded from neurons that exhibited DII morphology. Of all the DII neurons from P0 mice tested, 6/7 neurons displayed ADPs. Two other neurons also had ADPs, but their morphology is unknown.

**Table 1. ADP recorded from P10–11 and adult duodenal neurons**

	P10–11	Adult
Amplitude (mV)	$45.4 \pm 3.7$ ( $n = 24$ )*	$20.7 \pm 6.5$ ( $n = 8$ )
Duration (ms)	$3300 \pm 1344$ ( $n = 22$ )	$160 \pm 80$ ( $n = 8$ )

ADP evoked by a single pulse stimulus on an internodal strand with membrane potential held at  $-100$  mV.

\* $P = 0.002$ ; data presented as means  $\pm$  SEM; 2/24 P10–11 neurons had ADPs that did not return to baseline and was therefore excluded from duration analysis.

ADPs were also found in 8/11 DII/AH neurons in the adult duodenum (Fig. 4F); none of the neurons recorded in the ileum had ADPs. ADPs recorded from P10–11 mice were significantly larger in amplitude compared to those recorded from adult duodenum ( $P = 0.002$ , Table 1). Although the mean duration of ADPs recorded from P10–11 mice was longer than those recorded in adults, the difference was not statistically significant ( $P = 0.2$ ).

At P10–11, ADPs were completely abolished in the presence of cadmium chloride ( $\text{Ca}^{2+}$  channel blocker,  $100 \mu\text{M}$ ,  $n = 6$ ; Fig. 5D–E). The AHPs displayed by some of these neurons ( $n = 4$ ) were also blocked by cadmium chloride, causing the neurons to fire repetitively (Fig. 5F).

In summary, the presence of ADPs appears to be a characteristic of AH/DII neurons in the duodenum, and the ADPs are much more prominent in postnatal neurons than adult neurons.

### Early postnatal S-type neurons were unipolar and displayed fEPSPs

At P10–11, 38/92 neurons did not display long AHPs following action potentials and/or displayed fEPSPs, and were therefore classified as S-type in electrophysiology (Fig. 3D). Twenty-two of these neurons were identified by biocytin labelling, and they all possessed a single long process (Fig. 3D). P10–11, S-type neurons displayed fEPSPs in response to stimulation ( $n = 28$ ), and this was often accompanied by an array of non-stimulus-locked fEPSPs (in 10/28 neurons). Only three neurons were impaled for long enough to perform pharmacological analysis. In these neurons, the maximum amplitude and total number of peaks of the non-stimulus-locked fEPSPs were greatly reduced, if not completely abolished, by hexamethonium ( $200 \mu\text{M}$ , nicotinic receptor blocker;  $n = 3$ ). The amplitude of stimulus-locked fEPSPs was unaffected, but their duration and the total number of peaks were reduced by hexamethonium ( $n = 3$ ; Fig. 5A–C; Table 2).

At P0, 16/25 neurons had no ADP/AHPs, and/or displayed fEPSPs. The morphology of 14 of these neurons

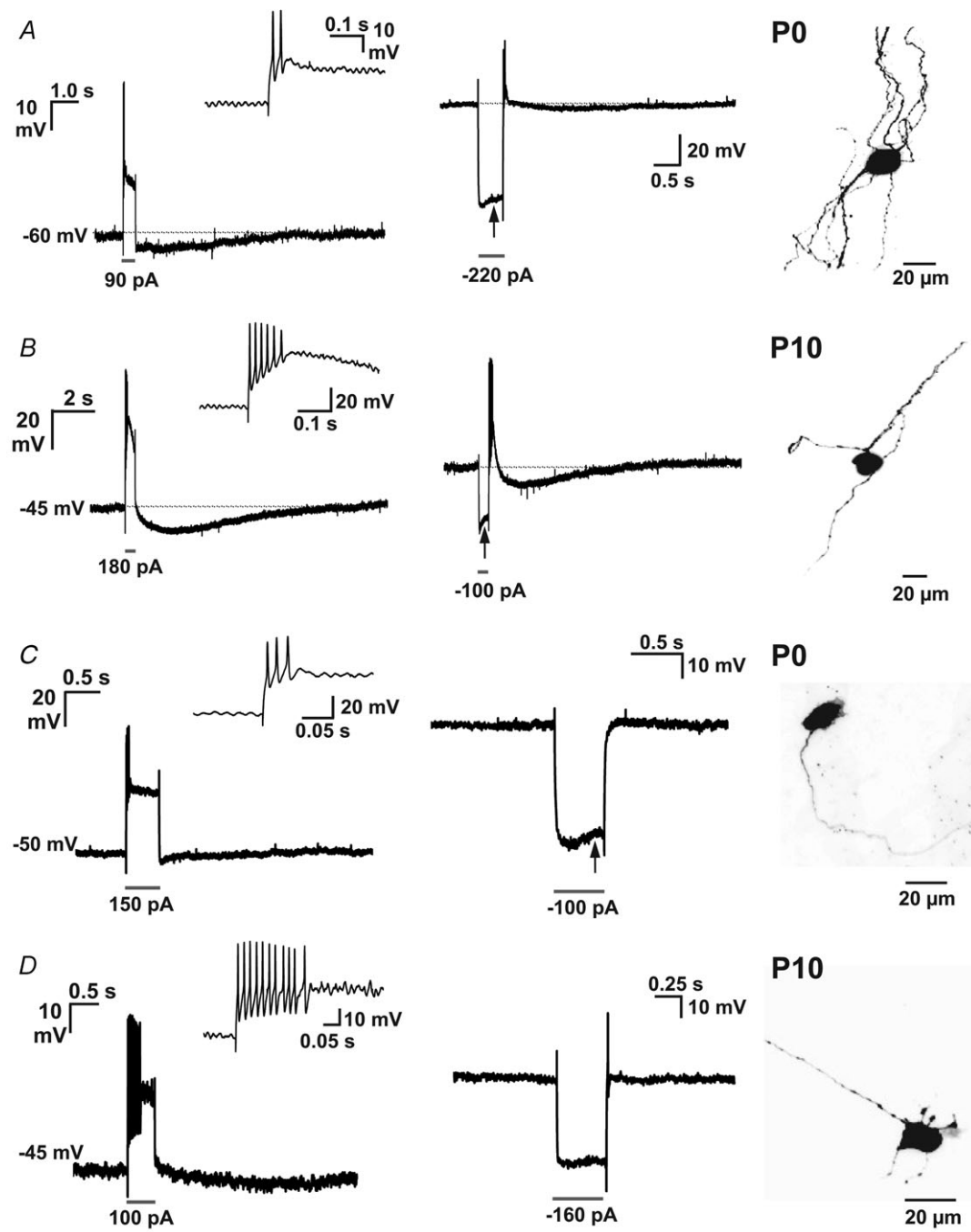


**Figure 3. Correlation of electrophysiological properties and morphology of postnatal neurons: DII neurons with prolonged AHPs and S-neurons with a single long process were present by P0**

Only one P0 neuron (A), but a group of neurons at P10–11 (B) had a prolonged AHP following a train of action potentials evoked by a 500 ms depolarizing step current, and they commonly exhibited an  $I_h$ -induced 'sag' in the membrane potential (arrows) response to a 500 ms hyperpolarizing pulse and anode break action potentials. These characteristics are typical of neurons exhibiting AH-type electrophysiology in the adult ENS. Neurons with prolonged AHPs at P0 and P10–11 displayed DII morphology (inverted confocal micrographs RHS). Another subgroup of neurons at P0 (C) and P10–11 (D) exhibited S-type electrophysiological properties. These neurons did not have a long AHP following action potentials, and rarely exhibited anode break action potentials and  $I_h$ -induced sag in the voltage (arrows) in response to prolonged hyperpolarizing pulse stimulus. Neurons with S-type electrophysiology at P0 and P10–11 only had one long process (inverted confocal micrographs RHS). All insets are enlarged representations of the electrophysiological traces. They reveal the action potentials evoked at the beginning of the depolarization step current stimulus.

was examined and they all had a single long process. Spontaneous fEPSPs were recorded from 8 out of the 16 neurons. In one neuron, application of hexamethonium completely abolished fEPSPs evoked by a single stimulus pulse.

Although fEPSPs were displayed by the majority of S-type neurons studied, a few AH-type neurons

also exhibited fEPSPs. In the adult duodenum, 18/19 uniaxonal neurons had fEPSPs, while 3/15 AH-type neurons displayed fEPSPs. The majority of S-type and some AH-type neurons in the adult ileum also had fEPSPs (data not shown). At P10–11, only 2/35 neurons with prolonged AHPs, and none of the P0 DII neurons displayed fEPSPs.

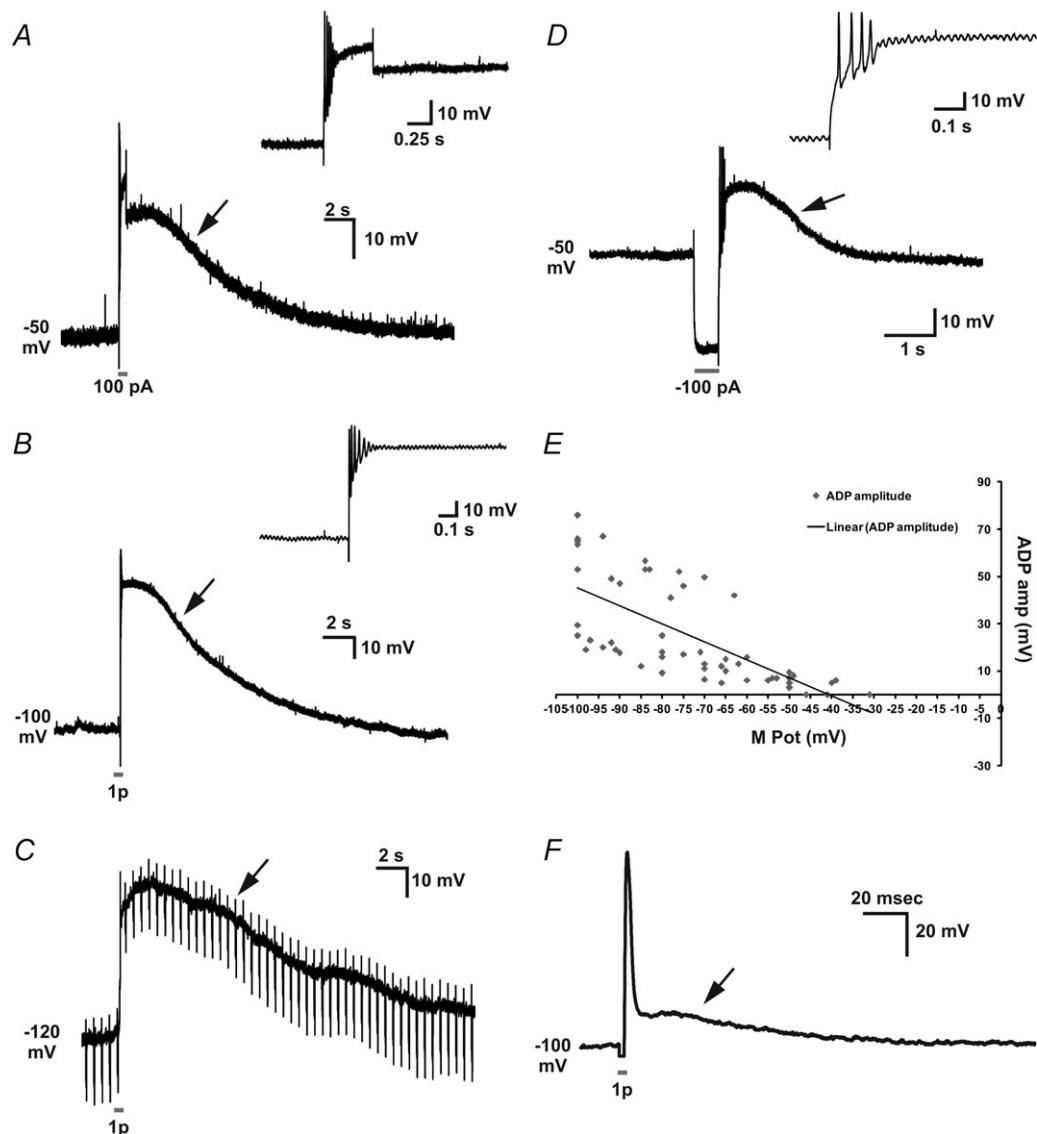


**Figure 4.** DII neurons in the duodenum exhibit an ADP that is very prominent at early postnatal ages

At P10–11, prominent ADPs (arrows) were observed following action potentials that were evoked by a 500 ms long depolarizing step current (A), at the end of a 500 ms long hyperpolarizing step current (D), or stimulation of an internodal strand (single pulse, 1.8 mA) (B–C). ADPs were only exhibited by neurons with DII morphology. Small action potentials can be evoked at the rising phase of an ADP. These ADPs (arrow) were associated with a decrease in input resistance (C), and have a reversal potential of  $-41$  mV (E). F, adult duodenal AH-type neurons also displayed an ADP (arrow) following an action potential evoked by a single pulse stimulus on an internodal strand. However adult ADPs were significantly smaller than the ADPs recorded from P10–11 neurons. All insets are enlarged representations of the electrophysiological traces and reveal the action potentials evoked at the beginning of a stimulus, as well as the initial stage of an ADP.

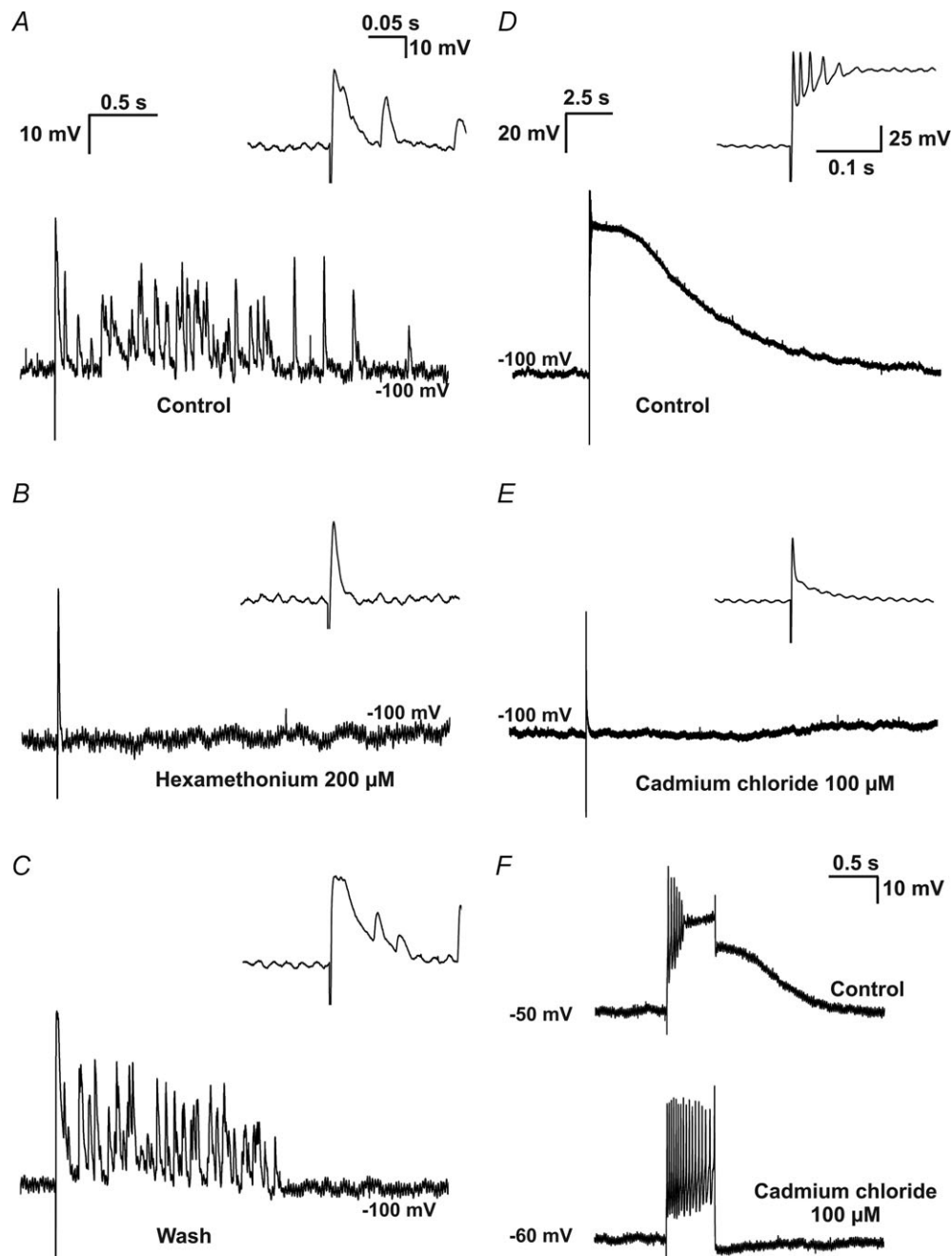


**Figure 5. Pharmacological analysis of electrically stimulated responses recorded from P10–11 neurons**

A–C, preliminary pharmacological analysis of fEPSPs recorded from P10–11 S-type neurons ( $n = 3$ ). A, S-type neurons displayed a fEPSP complex in response to a single pulse stimulus on an internodal strand. This was often accompanied by an array of non-stimulus-locked fEPSPs. B, The non-stimulus-locked fEPSPs were reduced ( $n = 2$ ) or abolished ( $n = 1$ ) by hexamethonium (nicotinic blocker,  $200 \mu\text{M}$ ). The duration, but not the amplitude, of the stimulus-locked fEPSPs was reduced by hexamethonium ( $n = 3$ ). C, the effects of hexamethonium were reversible with wash-out. D, AH-type neurons exhibited a prominent ADP following an action potential evoked by a single pulse stimulus on an internodal strand. E, the ADP was completely abolished by cadmium chloride ( $\text{Ca}^{2+}$  channel blocker,  $100 \mu\text{M}$ ;  $n = 6$ ). F, cadmium chloride also abolished the long AHP displayed by some of these neurons ( $n = 4$ ) causing them to convert from a phasic pattern of action potential firing to tonic firing (firing action potentials throughout the length of a 500 ms depolarizing step current). All insets are enlarged representations of the electrophysiological traces and reveal the stimulus-evoked fast EPSPs (A–C), or action potentials evoked at the beginning of a stimulus, and also the initial stage of an ADP (D–E).

**Table 2. Effects of hexamethonium on fEPSPs from P10–11 S-type neurons ( $n = 3$ )**

fEPSPs	Treatment	Max amp (mV)	No. of peaks	Duration (ms)
Stimulus locked	Control	$31.3 \pm 2.5$	$3.3 \pm 1.1$	$78.3 \pm 14.9$
	Hex	$31.0 \pm 4.4$	$1.5 \pm 0.6$	$47.0 \pm 12.0$
Non-stimulus locked	Control	$15.1 \pm 4.8$	$7.0 \pm 2.5$	
	Hex	$6.6 \pm 5.0$	$1.7 \pm 1.5$	

Hex, hexamethonium (200  $\mu\text{M}$ ); Max amp, maximum amplitude.

### Slow EPSPs were rare in postnatal neurons

In the adult duodenum, 11/15 uniaxonal, and 2/7 DII neurons displayed slow EPSPs. Slow EPSPs were recorded from every neuron examined in the adult ileum (uniaxonal: 5/5; DII: 2/2). However, slow EPSPs were observed in only one neuron (a P10–11 neuron with prolonged AHP) of all the early postnatal neurons examined ( $n = 46$ , tested with 3 and/or 10 stimulus trains).

### Comparison of electrophysiological properties across ages

The electrophysiological properties of neurons at different ages are summarized in Table 3. The resting membrane potential of P10–11 neurons was significantly more depolarized than adult neurons (P10–11 compared to adults,  $P < 0.0001$ ). The input resistance of P0 neurons recorded was significantly larger compared to P10–11s; and the input resistance of P10–11 neurons was significantly larger compared to adults ( $P < 0.0001$ , Table 2). This is consistent with an increase in the size of the soma of these neurons with age.

Adult AH neurons ( $P = 0.01$ ) and P10–11 neurons with prolonged AHPs ( $P = 0.01$ ) fired significantly more action potentials than adult and P10–11 S-type neurons. Eight S-neurons at P10–11 were examined for their firing properties; however, firing frequency comparisons between S-neurons and neurons with prolonged AHPs at this age were unreliable as 4/8 S-neurons only fired one action potential. At P10–11, S-neurons with a single long process ( $P = 0.006$ ) and neurons with prolonged AHPs ( $P < 0.0001$ ) had significantly lower instantaneous frequencies than adult S/uniaxonal and AH/DII neurons respectively. Neurons with prolonged AHPs at P10–11 had a significantly lower total burst frequency than adult AH neurons. Although a similar trend was observed for the total burst frequency between P10–11 S-neurons and adult S-neurons, this difference was not significant ( $P = 0.06$ ). In adults, the instantaneous frequency ( $P = 0.001$ ) and total burst frequency ( $P = 0.0001$ ) were greater in S-neurons compared to AH neurons. A greater proportion of AH-type neurons displayed an  $I_h$ -induced 'sag' in the membrane potential response to a prolonged hyperpolarizing pulse and anode break action potentials

compared to S-type neurons (both  $P < 0.0001$ ,  $\chi^2$  test, 1 df) at P10–11, but this was not observed in adults. An obvious sag in the voltage response to hyperpolarising current was observed in every P10–11 AH-type neuron examined ( $n = 29$ ; Fig. 3A–B); however an  $I_h$  was only found in 10/18 adult AH neurons ( $P = 0.0004$ ,  $\chi^2$  test, 1 df). A greater proportion of AH-type neurons displayed anode break action potentials at P10–11 compared to adult ( $P = 0.02$ ,  $\chi^2$  test, 1 df; Table 3).

P10–11, neurons with prolonged AHPs exhibited action potentials with smaller amplitudes and greater half-widths than their adult counterparts (Table 3). A group of AH-type neurons exhibited small amplitude action potentials with sizes of 30 mV and below ( $n = 6$ ); these neurons were excluded from further analysis. All adult AH-type neurons had a slight inflection, on the falling phase of their action potentials, which was assumed to be due to voltage-dependent  $\text{Ca}^{2+}$  channel activation; however, this inflection was not evident in neurons examined at P10–11.

### Discussion

The electrophysiological and morphological properties of duodenal neurons in an intact ENS were compared between three developmental ages: P0, P10–11 and adult. Neurons with multiple long processes (DII) and neurons with a single long process were present at birth; however, postnatal DII neurons showed differences in electrophysiological properties from adult neurons, including the presence of a prominent ADP, which served as an electrophysiological indicator of these neurons, especially at P0. The circumferential projections of DII neurons were mature by P10–11, whereas neurons with a single long process underwent significant changes in projection lengths and morphology between P10–11 and adult. In contrast to their morphological development, most electrophysiological characteristics of neurons with a single long process appeared to be mature by P10–11, before DII neurons.

### Morphological development of myenteric neurons

In the myenteric plexus of the adult mouse intestine, neurons can be broadly classified into neurons that have

Table 3. Electrophysiological properties of AH- and S-type duodenal neurons

AH-type	Age	RMP (mV)	$R_{in}$ (M $\Omega$ )	AP thres (pA)	Max no. of APs	Pres AHP	Pres ab-APs	Pres $I_h$	AP amp (mV)	AP half-width (ms)	Inst freq (Hz)	Total burst freq (Hz)
AH-type	P0	-42 (n = 1)	352 $\pm$ 16 (n = 5)									
	P10	-47 $\pm$ 1* (n = 33)	292 $\pm$ 16* (n = 27)	107 $\pm$ 8 (n = 35)	5.9 $\pm$ 0.3# (n = 35)	n = 20/22	n = 26/29##† (89.7%)	n = 29/29*^ (100%)	55 $\pm$ 3 (n = 11)	2.4 $\pm$ 0.1 (n = 11)	42 $\pm$ 2* (n = 35)	51 $\pm$ 2^ (n = 35)
	Adult	-58.2 $\pm$ 1.5 (n = 18)	192 $\pm$ 12 (n = 18)	111 $\pm$ 25 (n = 13)	4.9 $\pm$ 0.9# (n = 14)	n = 10/13	n = 10/18 (56%)	n = 10/18 (56%)	67 $\pm$ 3 (n = 18)	1.7 $\pm$ 0.1 (n = 15)	70 $\pm$ 6† (n = 12)	78 $\pm$ 13§ (n = 12)
S-type	P0	-43 $\pm$ 6 (n = 4)	348 $\pm$ 8 (n = 3)									
	P10	-39 $\pm$ 2 (n = 8)	285 $\pm$ 26 (n = 9)	103 $\pm$ 42 (n = 35)	3.4 $\pm$ 1.4 (n = 8)	None (n = 13)	n = 3/13 (23%)	n = 3/13 (23%)			58 $\pm$ 11^ (n = 4)	92 $\pm$ 34 (n = 4)
	Adult	-49.7 $\pm$ 0.9 (n = 20)	171 $\pm$ 13 (n = 19)	162 $\pm$ 15 (n = 18)	2.3 $\pm$ 0.5 (n = 20)	None (n = 20)	n = 7/20 (35%)	n = 7/20 (35%)			118 $\pm$ 11 (n = 14)	171 $\pm$ 16 (n = 14)

Ab, anode break; AP, action potential; freq, frequency; Inst, instantaneous; Pres, presence of;  $R_{in}$ , input resistance; RMP, resting membrane potential; thres, threshold; \*  $P < 0.0001$ ; §  $P = 0.0001$ ; †  $P = 0.001$ ; #  $P = 0.01$ ; ^  $P < 0.01$ ; ‡  $P < 0.05$ .

only one axon and neurons with multiple long axons, termed DII morphology (Furness *et al.* 2004; Nurgali *et al.* 2004; Qu *et al.* 2008; Sibaev *et al.* 2009). In the guinea-pig ileum, DII neurons have been shown to act as intrinsic sensory neurons (Kunze *et al.* 1995; Bertrand *et al.* 2000), and all their long processes function as axons (Hendriks *et al.* 1990). Uniaxonal neurons comprise multiple types of interneurons and motor neurons (Furness *et al.* 2004; Qu *et al.* 2008).

To our knowledge, the present study is the first to report the presence of DII neurons during ENS development. Although neurons with a single, long, anally projecting process are present in the gut from mid-embryonic (E11.5) stages (Young *et al.* 2002), there have not yet been any reports of DII neurons during prenatal development. However, the techniques used in the studies of prenatal development were not favourable for identifying circumferentially projecting neurons because the DiI crystals used to label the neurons were large relative to the circumference of the gut (Young *et al.* 2002). In the mouse intestine, DII neurons can also be detected by their immunoreactivity for calcitonin gene-related peptide (CGRP) (Furness *et al.* 2004; Qu *et al.* 2008). CGRP-expressing neurons are first detected in the mouse small intestine at E17 and later in the colon (Branchek & Gershon, 1989). Combined, the data suggest that DII neurons do not develop until late in embryonic development.

### **The increase in length of projections of DII neurons and neurons with a single long process does not parallel the increase in circumference or length of the gut**

The length and circumference of the mouse small intestine both grow significantly after birth. DII neurons achieved adult circumferential projection lengths by P10–11, and at this age, some DII neurons projected around almost the entire circumference of the gut. In contrast, the processes of DII neurons in the adult ENS project over only a fraction of the circumference. Assuming that the network of myenteric ganglia is stable after birth, our data suggest that the number of ganglia that an individual DII neuron supplies decreases after P10–11. Thus, as in the CNS (Takahashi, 2005; Lu *et al.* 2009; Blankenship & Feller, 2010), it appears likely that there are changes in the post-synaptic targets of at least some enteric neurons during development.

A DiI retrograde labelling study reported that orally projecting enteric neurons were only rarely observed before birth (Young *et al.* 2002). We found that at P0, neurons with a single long process that projected orally or anally were present. In contrast to DII neurons, the projection lengths of these neurons at P10–11 were

still significantly shorter than adult uniaxonal neurons. Moreover, the rate of increase in projection lengths of neurons with a single long process between P0 and P10–11 was lower than the rate of increase in the length of the small intestine. This might be because some subpopulations of neurons only start projecting their processes after birth. In the mouse, progenitors of several neuronal subtypes only exit the cell cycle late in embryonic development (Pham *et al.* 1991; Li *et al.* 2011). A previous study in the guinea pig reported postnatal changes in the proportions of different types of enteric neurons, suggesting that some classes of neurons only develop postnatally (Patel *et al.* 2010).

### **The morphology of neurons with a single long process undergoes significant changes during post-natal development**

In the colon (Nurgali *et al.* 2004) and duodenum (current study) of adult mice, the majority of uniaxonal neurons have lamellar dendrites only (DI morphology) or lamellar plus filamentous dendrites. In contrast, we showed that most neurons with a single long process in P0 mice possessed multiple filamentous neurites, and neurons with only lamellar neurites were rare. This is consistent with a previous study that reported only filamentous neurons in the gut of embryonic mice (Young *et al.* 2002). In the adult ENS, neurons with lamellar dendrites often receive synaptic inputs predominantly onto their dendrites (Pompolo & Furness, 1995; Young & Furness, 1995). As lamellar dendrite-like neurites develop after birth, it appears that many synaptic connections must develop after birth and/or significant synaptic remodelling occurs during early postnatal stages. Future ultrastructural studies are required to determine whether the filamentous neurites present transiently during development are the sites of synaptic inputs. There are also many reports of changes in dendritic morphology of CNS-neurons during development (Bailey *et al.* 2011; Emoto, 2011; Tavanoanis, 2011).

### **DII neuron and S-neurons with a single long process are present by P0**

The presence of neurons displaying AH-type electrophysiology (with characteristic long AHP following an action potential), and S-type electrophysiology during the development of the ENS has not previously been examined.

In the guinea-pig duodenum, AH-type neurons have a prominent inflection on the falling phase of their action potentials, known as the  $\text{Ca}^{2+}$  hump (Clerc *et al.* 1998). They also exhibit a large and prolonged AHP following an action potential evoked with a single pulse stimulus (Clerc *et al.* 1998). In the current study, no prominent

$\text{Ca}^{2+}$  humps were observed at P10–11; however, a group of neurons with DII morphology displayed prolonged AHPs typically only following a train of action potentials. The lack of a  $\text{Ca}^{2+}$  hump or obvious AHP following a single action potential at P10–11 is probably not surprising, as in adult mouse duodenal AH neurons, the  $\text{Ca}^{2+}$  hump is not as prominent, and the AHP is smaller, than in the guinea-pig (Clerc *et al.* 1998). At P0, only one neuron had a noticeable AHP following a train of action potentials, and this neuron had DII morphology. The scarcity of AHPs recorded at P0 could be partly or entirely due to the presence of a very prominent ADP in postnatal DII neurons (discussed below), which may have masked the AHP.

AH/DII neurons are thought to be intrinsic primary afferent neurons that are responsible for sensing the intestinal contents and stimulating propulsive motility patterns (Furness, 2006). Therefore, it might be expected that AH/DII neurons are required for neurally mediated motility. The presence of neurons with DII morphology, as well as orally and anally projecting S-neurons, by P0 is consistent with a previous study showing that spontaneous neurally mediated motility patterns in the mouse duodenum first appear just prior to birth (Roberts *et al.* 2010).

### Postnatal DII neurons have a prominent ADP

ADPs following action potentials were displayed by neurons with prolonged AHPs, and/or DII morphology in the duodenum of P0, P10–11 and adult mice. None of the AH-type neurons in the adult ileum had ADPs. ADPs have also been reported in AH neurons in the adult guinea-pig duodenum, where they are mediated by monovalent cations activated by  $\text{Ca}^{2+}$  entry via N-type  $\text{Ca}^{2+}$  channels (Vogalis *et al.* 2002).

The ADP displayed by P0 and P10–11 neurons was much more prominent than that recorded from adult neurons. At P10–11, the ADPs were completely abolished by the  $\text{Ca}^{2+}$  channel blocker, cadmium chloride, and the reversal potential of  $-41$  mV indicates that the underlying current probably involves a combination of ions. The functional significance of a prominent ADP in postnatal DII neurons is not yet known. Prominent  $\text{Ca}^{2+}$ -mediated events also occur in many parts of the developing CNS (Spitzer, 2006), and have been suggested to modulate the formation of synaptic connections (Leinekugel *et al.* 1998; Stocca *et al.* 2008).

### Fast excitatory synapses are the first functional synapses in the ENS

Little information is available about the development of synaptic transmission in the ENS. E11.5 enteric neurons cultured for 24 h exhibit calcium transients in response to

nicotinic agonists and ATP demonstrating the expression of some of the receptors involved in synaptic transmission in the mature ENS (Hao *et al.* 2011). Electron microscopy revealed rare ‘synapse-like’ contacts in the stomach of E12.5 mice. At E18.5, more mature synapses are present, and molecules associated with synapses such as synaptophysin are expressed (Vannucchi & Fausone-Pellegrini, 2000). As neurally mediated motility commences at E18.5 (Roberts *et al.* 2010), these data suggest that, while immature neurons may be electrically active from mid embryonic stages, the neuronal circuitry regulating motility is not functional until just prior to birth. In the current study, we provide the first evidence for functional synapses during ENS development as S-type neurons at both P0 and P10–11 displayed fEPSPs in response to electrical stimulation. Although it was only possible to examine the pharmacology of the fEPSPs in three neurons, like adult neurons, the fEPSPs in postnatal neurons were predominantly mediated by acetylcholine acting at nicotinic receptors. The hexamethonium-resistant component of the fEPSP suggests the involvement of another neurotransmitter, such as ATP, which has been shown to mediate some fEPSPs in the mouse gut (Nurgali *et al.* 2004).

In the adult mouse, slow EPSPs are observed in both S-type and AH-type neurons (Nurgali *et al.* 2004; Gwynne & Bornstein, 2007). Slow EPSPs were only recorded from one neuron at P10–11 and were not observed at P0. However, because the presence of hyoscine was essential in order to hold the impalements of P0 and P10–11 neurons, we cannot rule out the possibility that a muscarinic contribution to slow EPSPs is present.

### Passive membrane properties and action potential properties mature with age

The passive membrane properties of enteric neurons, including input resistance and resting membrane potential, changed during development. This is similar to what is observed in other parts of the developing nervous systems (Picken Bahrey & Moody, 2003; Tu *et al.* 2003; Ambrogini *et al.* 2004; Moe *et al.* 2005), and probably reflects increases in soma size and in the densities of ion channels with maturity.

### Conclusions

Previous studies of guinea-pig, rat and human have reported postnatal changes in the proportions of different types of enteric neurons and in enteric neuromuscular transmission (de Vries *et al.* 2010; Patel *et al.* 2010; Wittmeyer *et al.* 2010). Our study, which is the first to examine developmental changes in electrophysiological and morphological properties of neurons in an intact ENS,

found that the main neuron types (DII and S-neurons with a single long process) comprising reflex pathways underlying the propulsive behaviour of the gut could be distinguished by P0. However, these neurons underwent significant changes in morphology and electrophysiology between postnatal stages and achieving their mature properties in adulthood. A notable example was the presence of a prominent  $\text{Ca}^{2+}$ -mediated ADP at P0 and P10–11 in DII neurons. We also provide the first direct evidence of functional synapses in the ENS at P0, although slow EPSPs were rarely observed in postnatal neurons, even at P10–11. Future studies are required to identify the effects on motility of the major developmental changes in the electrophysiological properties of enteric neurons we have documented.

## References

- Ambrogini P, Lattanzi D, Ciuffoli S, Agostini D, Bertini L, Stocchi V, Santi S & Cuppini R (2004). Morpho-functional characterization of neuronal cells at different stages of maturation in granule cell layer of adult rat dentate gyrus. *Brain Res* **1017**, 21–31.
- Baetge G & Gershon MD (1989). Transient catecholaminergic (TC) cells in the vagus nerves and bowel of fetal mice – relationship to the development of enteric neurons. *Dev Biol* **132**, 189–211.
- Bailey CD, Alves NC, Nashmi R, De Biasi M & Lambe EK (2011). Nicotinic  $\alpha 5$  subunits drive developmental changes in the activation and morphology of prefrontal cortex layer VI neurons. *Biol Psychiatry* **71**, 120–128.
- Bertrand PP, Kunze WAA, Furness JB & Bornstein JC (2000). The terminals of myenteric intrinsic primary afferent neurons of the guinea-pig ileum are excited by 5-hydroxytryptamine acting at 5-hydroxytryptamine-3 receptors. *Neuroscience* **101**, 459–469.
- Blankenship AG & Feller MB (2010). Mechanisms underlying spontaneous patterned activity in developing neural circuits. *Nat Rev Neurosci* **11**, 18–29.
- Bornstein JC, Furness JB & Kunze WAA (1994). Electrophysiological characterization of myenteric neurons – how do classification schemes relate. *J Auton Nervous Syst* **48**, 1–15.
- Branchek TA & Gershon MD (1989). Time course of expression of neuropeptide-Y, calcitonin gene-related peptide, and NADPH diaphorase activity in neurons of the developing murine bowel and the appearance of 5-hydroxytryptamine in mucosal enterochromaffin cells. *J Comp Neurol* **285**, 262–273.
- Clerc N, Furness JB, Bornstein JC & Kunze WAA (1998). Correlation of electrophysiological and morphological characteristics of myenteric neurons of the duodenum in the guinea-pig. *Neuroscience* **82**, 899–914.
- de Vries P, Soret R, Suply E, Heloury Y & Neunlist M (2010). Postnatal development of myenteric neurochemical phenotype and impact on neuromuscular transmission in the rat colon. *Am J Physiol Gastrointest Liver Physiol* **299**, G539–G547.
- Drummond GB (2009). Reporting ethical matters in *The Journal of Physiology*: standards and advice. *J Physiol* **587**, 713–719.
- Emoto K (2011). Dendrite remodeling in development and disease. *Dev Growth Differ* **53**, 277–286.
- Furness JB (2006). *The Enteric Nervous System*. Blackwell Publishing, Malden, MA, USA.
- Furness JB, Kunze WAA, Bertrand PP, Clerc N & Bornstein JC (1998). Intrinsic primary afferent neurons of the intestine. *Progr Neurobiol* **54**, 1–18.
- Furness JB, Robbins HL, Xiao JH, Stebbing MJ & Nurgali K (2004). Projections and chemistry of Dogiel type II neurons in the mouse colon. *Cell Tissue Res* **317**, 1–12.
- Gershon MD (1998). *The Second Brain*. Harper Collins Publishers, New York.
- Gershon MD (2010). Developmental determinants of the independence and complexity of the enteric nervous system. *Trends Neurosci* **33**, 446–456.
- Gwynne RM & Bornstein JC (2007). Synaptic transmission at functionally identified synapses in the enteric nervous system: Roles for both ionotropic and metabotropic receptors. *Curr Neuroparmacol* **5**, 1–17.
- Hao MM, Boesmans W, Van den Abbeel V, Jennings EA, Bornstein JC, Young HM & Vanden Berghe P (2011). Early emergence of neural activity in the developing mouse enteric nervous system. *J Neurosci* **31**, 15352–15361.
- Hao MM & Young HM (2009). Development of enteric neuron diversity. *J Cell Mol Med* **13**, 1193–1210.
- Hendriks R, Bornstein JC & Furness JB (1990). An electrophysiological study of the projections of putative sensory neurons within the myenteric plexus of the guinea pig ileum. *Neurosci Lett* **110**, 286–290.
- Hirst GDS, Holman ME & Spence I (1974). Two types of neurons in myenteric plexus of duodenum in guinea-pig. *J Physiol* **236**, 303–326.
- Kapur RP, Yost C & Palmiter RD (1992). A transgenic model for studying development of the enteric nervous-system in normal and aganglionic mice. *Development* **116**, 167–175.
- Kunze WAA, Bornstein JC & Furness JB (1995). Identification of sensory nerve-cells in a peripheral organ (the intestine) of a mammal. *Neuroscience* **66**, 1–4.
- Langley JN (1921). *The Autonomic Nervous System*. W. Heffer and Sons, Cambridge, UK.
- Leinekugel X, Khalilov I, Ben-Ari Y & Khazipov R (1998). Giant depolarizing potentials: the septal pole of the hippocampus paces the activity of the developing intact septohippocampal complex in vitro. *J Neurosci* **18**, 6349–6357.
- Li Z, Chalazonitis A, Huang YY, Mann JJ, Margolis KG, Yang QM, Kim DO, Cote F, Mallet J & Gershon MD (2011). Essential roles of enteric neuronal serotonin in gastrointestinal motility and the development/survival of enteric dopaminergic neurons. *J Neurosci* **31**, 8998–9009.
- Lu B, Wang KH & Nose A (2009). Molecular mechanisms underlying neural circuit formation. *Curr Opin Neurobiol* **19**, 162–167.
- Moe MC, Varghese M, Danilov AI, Westerlund U, Ramm-Petersen J, Brundin L, Svensson M, Berg-Johnsen J & Langmoen IA (2005). Multipotent progenitor cells from the adult human brain: neurophysiological differentiation to mature neurons. *Brain* **128**, 2189–2199.

- Nurgali K, Stebbing MJ & Furness JB (2004). Correlation of electrophysiological and morphological characteristics of enteric neurons in the mouse colon. *J Comp Neurol* **468**, 112–124.
- Patel BA, Dai X, Burda JE, Zhao H, Swain GM, Galligan JJ & Bian X (2010). Inhibitory neuromuscular transmission to ileal longitudinal muscle predominates in neonatal guinea pigs. *Neurogastroenterol Motil* **22**, 909–918, e236–237.
- Pham TD, Gershon MD & Rothman TP (1991). Time of origin of neurons in the murine enteric nervous-system – sequence in relation to phenotype. *J Comp Neurol* **314**, 789–798.
- Picken Bahrey HL & Moody WJ (2003). Early development of voltage-gated ion currents and firing properties in neurons of the mouse cerebral cortex. *J Neurophysiol* **89**, 1761–1773.
- Pompolo S & Furness JB (1995). Sources of inputs to longitudinal muscle motor-neurons and ascending interneurons in the guinea-pig small-intestine. *Cell Tissue Res* **280**, 549–560.
- Qu ZD, Thacker M, Castelucci P, Bagyanszki M, Epstein M & Furness J (2008). Immunohistochemical analysis of neuron types in the mouse small intestine. *Cell Tissue Res* **334**, 147–161.
- Roberts RR, Ellis M, Gwynne RM, Bergner AJ, Lewis MD, Beckett EA, Bornstein JC & Young HM (2010). The first intestinal motility patterns in fetal mice are not mediated by neurons or interstitial cells of Cajal. *J Physiol* **588**, 1153–1169.
- Roberts RR, Murphy JF, Young HM & Bornstein JC (2007). Development of colonic motility in the neonatal mouse-studies using spatiotemporal maps. *Am J Physiol Gastrointest Liver Physiol* **292**, G930–G938.
- Sibaev A, Yuce B, Kemmer M, Van Nassauw L, Broedl U, Allescher HD, Goke B, Timmermans JP & Storr M (2009). Cannabinoid-1 (CB<sub>1</sub>) receptors regulate colonic propulsion by acting at motor neurons within the ascending motor pathways in mouse colon. *Am J Physiol Gastrointest Liver Physiol* **296**, G119–G128.
- Spitzer NC (2006). Electrical activity in early neuronal development. *Nature* **444**, 707–712.
- Stocca G, Schmidt-Hieber C & Bischofberger J (2008). Differential dendritic Ca<sup>2+</sup> signalling in young and mature hippocampal granule cells. *J Physiol* **586**, 3795–3811.
- Takahashi T (2005). Postsynaptic receptor mechanisms underlying developmental speeding of synaptic transmission. *Neurosci Res* **53**, 229–240.
- Tavosanis G (2011). Dendritic structural plasticity. *Dev Neurobiol* **72**, 73–86.
- Tu YL, Liu YB, Zhang L, Zhao YJ, Wang L & Hu ZA (2003). [Changes in electrophysiological and morphological properties of neurons during the development of the visual cortex in the rat]. *Sheng Li Xue Bao* **55**, 206–212.
- Vannucchi MG & Fausone-Pellegrini MS (2000). Synapse formation during neuron differentiation: An in situ study of the myenteric plexus during murine embryonic life. *J Comp Neurol* **425**, 369–381.
- Vogalis F, Harvey JR, Lohman RJ & Furness JB (2002). Action potential afterdepolarization mediated by a Ca<sup>2+</sup>-activated cation conductance in myenteric AH neurons. *Neuroscience* **115**, 375–393.
- Wittmeyer V, Merrot T & Mazet B (2010). Tonic inhibition of human small intestinal motility by nitric oxide in children but not in adults. *Neurogastroenterol Motil* **22**, 1078–e282.
- Young HM, Ciampoli D, Hsuan J & Canty AJ (1999). Expression of Ret-, p75(NTR)-, Phox2a-, Phox2b-, and tyrosine hydroxylase-immunoreactivity by undifferentiated neural crest-derived cells and different classes of enteric neurons in the embryonic mouse gut. *Dev Dyn* **216**, 137–152.
- Young HM & Furness JB (1995). Ultrastructural examination of the targets of serotonin-immunoreactive descending interneurons in the guinea pig small intestine. *J Comp Neurol* **356**, 101–114.
- Young HM, Jones BR & McKeown SJ (2002). The projections of early enteric neurons are influenced by the direction of neural crest cell migration. *J Neurosci* **22**, 6005–6018.

### Author contributions

The work has been conducted in the laboratories headed by J.B.F., J.C.B. and H.M.Y. J.P.P.F.: conception and design, collection, analysis and interpretation of data, manuscript writing; T.V.N.: design of experiments, collection, analysis and interpretation of data; J.B.F.: conception and design, analysis and interpretation of data, manuscript revision; J.C.B.: conception and design, analysis and interpretation of data, manuscript revision; H.M.Y.: conception and design, analysis and interpretation of data, manuscript preparation and revision. All authors have approved the final version of the manuscript.

### Acknowledgements

This work was supported by the Australian Research Council Discovery Grant DP0878755 (HMY/JCB) and NHMRC Project Grant 566642 (JCB). We thank Annette Bergner and Yan Hong Tan for technical assistance, and Colin Anderson and Rachel Gwynne for their invaluable suggestions.